JOURNAL OF CATALYSIS 152, 350–359 (1995)

Effects of Sodium on the Structure and Fischer–Tropsch Synthesis Activity of Ru/TiO_2

Takashi Komaya,*[,1] Alexis T. Bell,* Zara Weng-Sieh,† Ronald Gronsky,† Frank Engelke,‡ Terry S. King,‡ and Marek Pruski‡

*Chemical Sciences Division, Lawrence Berkeley Laboratory, and Department of Chemical Engineering, University of California, Berkeley, California 94720; †Materials Science Division, Lawrence Berkeley Laboratory, and Department of Materials Science and Mineral Engineering, University of California, Berkeley, California 94720; and ‡Institute of Physical Research and Technology, Ames Laboratory, and Department of Chemical Engineering Iowa State University, Ames, Iowa 50011

Received August 18, 1994; revised November 3, 1994

The influence of Na on the migration of Ti-containing moieties onto the surface of Ru particles supported on titania has been investigated, together with the effects of Na on the activity and selectivity of titania-supported Ru for Fischer–Tropsh synthesis. It is demonstrated that Na facilitates the decoration and partial encapsulation of Ru by Ti-containing moieties as a consequence of the formation of sodium titanates. Since the Tammann temperature of the titanates is lower than that of the anatase or rutile phases of titania, the temperature at which Ti-containing moieties begin to migrate is reduced in the presence of Na. The turnover frequency for CO consumption based on exposed Ru sites is observed to be independent of the Na content of the catalyst, but the turnover frequency for methane formation decreases monotonically with increasing Na content. The probability for chain growth and the olefin-to-paraffin ratio increase and the extent of ethylene reincorporation into the reaction products decrease with increasing Na content. These effects are attributed to a reduction in the surface concentration and mobility of H atoms adsorbed on Ru.

INTRODUCTION

Ruthenium exhibits a high intrinsic activity for Fischer–Tropsch synthesis (FTS) and a high selectivity for linear α olefins [see for example Ref. (1)]. Both the activity and selectivity of Ru can be influenced by the composition of the support (2–6). For a given Ru particle size and set of reaction conditions, as much as a 10-fold higher activity is reported when titania rather than silica or alumina is used as the support. Similarly, the products obtained over titania-supported Ru exhibit a higher average molecular weight and olefin-to-paraffin ratio for a given set of reaction conditions. The effects of titania on the activity and selectivity of Ru and other transition metals used for FTS have been attributed to decoration or partial encapsulation of the supported metal particles by TiO_x moieties derived from the support (2–8).

We have recently shown that the coverage of titania-supported Ru particles by TiO_x can be determined quantitatively and have investigated the effects of titania coverage on catalyst activity and selectivity (9, 10). The average size of the supported Ru crystallites was determined from TEM micrographs, and the fraction of the Ru particle surface available for H_2 chemisorption was determined by ^1H NMR. The TEM micrographs revealed that the portion of the Ru surface unavailable for H_2 adsorption is covered by a thin layer of amorphous titania. As the fraction of the Ru particle surface covered by titania increases, the turnover frequency for CO consumption, based on the surface area available for H_2 adsorption, increases and passes through a maximum at a titania coverage of about 0.5. The turnover frequency for methane formation decreases monotonically with increasing titania coverage, whereas the probability for chain growth, α, and the olefin-to-paraffin ratio both increase. The higher activity of titania-supported Ru is attributed to the formation of exceptionally active sites at the boundary between the metal and the titania overlayer (3–8, 10). At metal sites adjacent to the titania, overlayer carbon monoxide can adsorb so that the carbon end of the molecule is bonded to the metal, while the oxygen end interacts with titanium cations exposed at the edge of the oxide. The latter interaction is representative of a Lewis acid-base interaction and contributes to the dissociation of the C–O bond, the first step in the hydrogenation of CO to methane and higher molecular weight hydrocarbons. The higher probability of chain growth and the higher olefin-to-paraffin ratio of products formed over titania-supported metals has been attributed to inhibition of hydrogen adsorption and diffusion on the metal surface (3–8).

[1] Present address: Production Technology and Engineering Center, Mitsubishi Kasei Corporation, Kurosaki, Yahata-nishi-ku, Kitakyushu, Fukuoka 806, Japan.

0021-9517/95 $6.00

The effects of alkali metal oxides on the activity and selectivity of silica- or alumina-supported Ru for FTS has also been investigated extensively (11–16). With increasing alkali promotion, the turnover frequency for CO consumption, based on CO adsorption, decreases, whereas the probability for chain growth and the olefin to paraffin ratio both increase. Alkali promotion of supported Ru markedly decreases the rate of dissociative CO adsorption (13, 15) and reduces the reactivity of surface carbon produced through CO dissociation (12). Potassium promotion of Ru physically blocks the metal sites available for H_2 chemisorption (17, 18).

The present investigation was undertaken with the aim of identifying the effects of sodium on the activity and selectivity of titania-supported Ru for FTS. This theme is of particular interest since it has been observed that small amounts of K added to titania-supported Pt suppress the adsorption of H_2 (19). This phenomenon has been attributed to the reaction of K_2O with TiO_2 to form various potassium titanates, e.g., K_2TiO_3, $K_2Ti_2O_5$, $K_2Ti_4O_9$, and $K_2Ti_6O_{13}$, all of which exhibit melting points, and hence Tammann temperatures, significantly lower than that of TiO_2. It is, therefore, argued that K_2O could act as flux which promoted the redistribution of titania over the surface of the supported Pt particles. The purpose of the investigation reported here is to determine the extent to which Na influences the coverage of Ru particles by Ti-containing moieties, as well as the turnover frequency for CO consumption, the probability of chain growth, and the olefin to paraffin ratio of the reaction products.

EXPERIMENTAL

Catalyst Preparation and Characterization

Na-containing Ru/TiO_2 catalysts were prepared by incipient wetness impregnation of TiO_2 (Degussa P-25) with an aqueous solution of $Ru(NO)(NO_3)_3$ (Johnson-Matthey) containing 5.4 wt% sodium as a contaminant. The impregnanted support was dried in air at 383 K for 16 h, and then sieved to 30–60 mesh size fractions. The dried catalyst was reduced at 543 K in a flow of H_2 and passivated by He containing 1000 ppm O_2 at room temperature and stored for future use. Na-free Ru/TiO_2 catalysts were prepared by washing the reduced Na-containing Ru/TiO_2 catalysts repeatedly in boiling water. The washed catalyst was dried at 383 K in vacuum for 3 h and then reduced in the same manner as Na-containing Ru/TiO_2. The weight loading of Ru was determined by X-ray fluorescence. The Na contents before and after boiling water wash were determined by ICP analysis. The chloride contents were below the detection limit (<0.02%) for all catalysts.

The dispersion of the supported Ru particles was determined by transmission electron microscopy (TEM) and the surface morphology of the support was characterized by scanning electron microscopy (SEM). TEM micrographs were obtained on a Topcon 002B transmission electron microscope operating at 200 keV. The average Ru particle size was determined from image-processing analysis of about 100 particles and the dispersion was determined from the average particle size (9, 10). SEM micrographs were obtained on a JEOL 35CF scanning electron microscope operating at between 12 and 15 kV.

All NMR experiments were performed on a home-built spectrometer operating at 250 MHz proton resonance frequency. The fraction of the Ru surface sites available for H_2 chemisorption was determined from ^1H NMR measurements by placing about 400 mg of catalyst, which had been used for FTS and then passivated in He containing 1000 ppm of O_2, in an *in situ* NMR probe attached to a volumetric adsorption apparatus. The sample was then reduced at 523 K for 2 h in 760 Torr H_2. After reduction, the sample was evacuated for 1 h at the reduction temperature and cooled to room temperature. The sample was then dosed with H_2 at 400 Torr, equilibrated for 30 min and evacuated to 10^{-5} Torr for 10 min.

Under the above conditions, the spectrum of H_2 adsorbed on Ru is characterized by resonances located between −30 to −70 ppm. For quantification of the amount of H_2 adsorbed on Ru, the observed signal is compared with that of water slightly doped with $FeCl_3$ (9). The fraction of the surface available for H_2 chemisorption is calculated as the ratio of H_i/Ru_{total} to Ru_s/Ru_{total}, where H_i is the moles of irreversibly adsorbed H_2 per gram of catalyst and Ru_s and Ru_{total} are the moles of surface and total Ru, respectively, per gram of catalyst. The fraction of the catalyst covered by TiO_x is given by $\theta_{TiO_x} = 1 - (H_i/Ru_s)$.

Selective excitation was accomplished by using a DANTE (delays alternating with nutations for tailored excitation) pulse sequence (20). In most experiments a pulse separation of 25 μs was chosen, resulting in a total duration of a DANTE sequence of 750 μs and the corresponding spectral excitation width of the centerband of ≈1.5 kHz. The excitation sidebands were separated from the centerband by 40 kHz and did not affect the NMR spectrum. The overall flip angle of the DANTE sequence was adjusted by varying the pulse width, while the rf amplitude remained constant. After a recovery period of at least 30 μs, a final 90° pulse was applied, followed by detection of the free induction decay. Additional details concerning the NMR experiments are given in Refs. (9, 21–23).

Reaction Apparatus

All reactions were carried out in a low dead volume quartz microreactor supplied with H_2, D_2, ^{12}CO, ^{13}CO, $^{12}C_2H_4$, and He from a gas manifold. UHP H_2 (Matheson Gas) and D_2 (Union Carbide) were further purified by

TABLE 1

Characteristics of Na-Containing and Na-Free Ru/TiO_2

Catalyst	Na-containing Ru/TiO_2			Na-free Ru/TiO_2		
	A1	B1	C1	A2	B2	C2
Ru (wt%)	1.52	4.70	6.60	1.52	4.76	6.65
Na (wt%)	0.33	1.00	1.70	0.01	0.03	0.02
D_{Ru}[a]	0.83	0.70	0.56	0.77	0.67	0.50
$H_{i,Ru}/Ru_{total}$[b]	0.14	0.07	0.05	0.38	0.34	0.28
θ_{TiO_x}[c]	0.83	0.90	0.91	0.51	0.49	0.44
$1 - \theta_{TiO_x}$	0.17	0.10	0.09	0.49	0.51	0.56
Enhancement in TiO_x coverage due to Na	1.64	1.82	2.07	1.00	1.00	1.00

[a] Ru dispersion determined from TEM images.
[b] Hydrogen uptake determined by 1 H NMR.
[c] $\theta_{TiO_x} = 1 - [(H_{i,Ru}/Ru_{total})/D_{Ru}]$.

passage through a Deoxo unit (Engelhard Industries) and water was removed by a molecular sieve 13X trap. UHP CO (99.999% pure, Matheson Gas) was passed through a glass bead trap maintained at 573 K to remove iron carbonyls, an Ascarite trap to remove CO_2, and a molecular sieve trap to remove water. ^{13}CO (Isotec Inc., 99% ^{13}C) and 2% ethylene in He (Matheson Gas) were used as supplied. The products obtained from the reaction of CO and H_2 (D_2) were analyzed by gas chromatography using a fused silica capillary column (0.25 mm i.d. × 50 m) coated with a 1-μm film of SE-54. For the experiments in which ^{13}CO, H_2, and $^{12}C_4H_4$ were fed to the reactor, product analysis was carried out by gas chromatography/mass spectrometry, as described in Ref. (24).

RESULTS AND DISCUSSION

The characteristics of Na-containing and Na-free Ru/TiO_2 are presented in Table 1. After boiling-water washing of the catalyst, only 1–3% of the contaminant Na remains. TEM analysis of the catalysts indicates that the removal of Na has little effect on the Ru particle size and, hence, dispersion. The TEM images of catalysts C1 and C2 are shown in Figs. 1 and 2, and SEM images of these two catalysts are shown in Fig. 3. Both TEM and SEM indicate that the surface of the titania is significantly rougher in the Na-containing sample (C1) than in the Na-free sample (C2). Selected area electron diffraction patterns of sample C1 show lattice reflections characteristic of the interplanar spacing of anatase (3.5 Å), the major component of Degussa P-25 titania, in addition to lattice reflections for interplanar spacings between 3.6 and 8.3 Å. The high-resolution TEM images presented in Fig. 1 reveal regions with lattice fringe spacings of 5.6 and 6.6 Å. Similar TEM images of sample C2 show no evidence for interplanar spacings larger than those characteristic of anatase. Table 1 shows that the presence of Na strongly affects the fraction of the Ru particle surface available for H_2 adsorption. For the Na-containing samples, only 0.09–0.17 of the Ru surface is available for H_2 adsorption. After boiling-water washing to remove Na, the fraction of the Ru surface available for H_2 adsorption increases to 0.49–0.56.

In related studies of Na-free Ru/TiO_2 (9), we have shown by means of TEM that the decrease in the fraction of the total Ru particle surface available for H_2 adsorption is attributable to a partial coverage or encapsulation of the Ru particle surfaces by an amorphous overlayer of TiO_x. The enhanced suppression of H_2 chemisorption for the Na-containing samples, reported in Table 1, is due to effects of Na on the encapsulation of Ru particles by moieties derived from the support. Na cations are known to substitute into the lattice of TiO_2, thereby forming a variety of sodium titanates ($Na_xTi_yO_z$) (25). Most of the interplanar spacings of these compounds are larger than those for anatase and lie in the range of 3.6 to 10 Å (see Table 2). The large interplanar spacings may, therefore, be ascribed to sodium titanate phases such as Na_2TiO_3, $Na_2Ti_4O_9$, $Na_2Ti_3O_7$, $Na_2Ti_5O_{11}$, $Na_2Ti_6O_{13}$, and $Na_2Ti_9O_{19}$, etc. Several of these anomalous reflections and fringes might also be attributable to the formation of sodium ruthenates such as Na_2RuO_3, Na_3RuO_4, or $Na_4Ru_3O_8$, but the apparent increased roughness of the titania support in the presence of sodium suggests the former scenario. Formation of sodium titanates is known to occur at temperatures as low as 523 K. Watanabe (26) has reported the formation of $Na_{0.23}TiO_2$, $Na_2Ti_4O_9$, and $Na_2Ti_9O_{19}$ upon reaction of TiO_2 with NaOH at 523 K, and the formation of $Na_2Ti_3O_7$ and $Na_2Ti_6O_{13}$ upon reaction

TABLE 2

Assignment of Observed Interplanar Spacings to Sodium Titanate and Sodium Ruthenate Phases

d_{hkl} (Å)[a]	$Na_xTi_yO_z$ ($x - y - z$)	$Na_xRu_yO_z$ ($x - y - z$)
8.26	2-4-9, 2-3-7	3-1-4
7.67	2-4-9, 2-6-13, 2-9-19, 2-5-11	
6.6	2-3-7	2-1-3
5.6	4-5-12, 0.23-1-2, 2-3-7, 1-1-2, 2-5-11, 2-4-9	2-4-9, 1-2-4
4.67	2-3-7, 2-9-19	2-1-3
3.9	2-4-9	3-1-4, 2-1-3
3.83	2-4-9, 2-9-19	4-3-8
3.7	2-6-13, 2-5,11	3-1-4, 4-3-8
3.58	2-9-19, 2-6-13	3-1-4, 2-1-3

[a] Observed interplanar lattice spacing determined from selected area diffraction patterns. The accuracy of the interplanar spacings is ±0.2 Å.

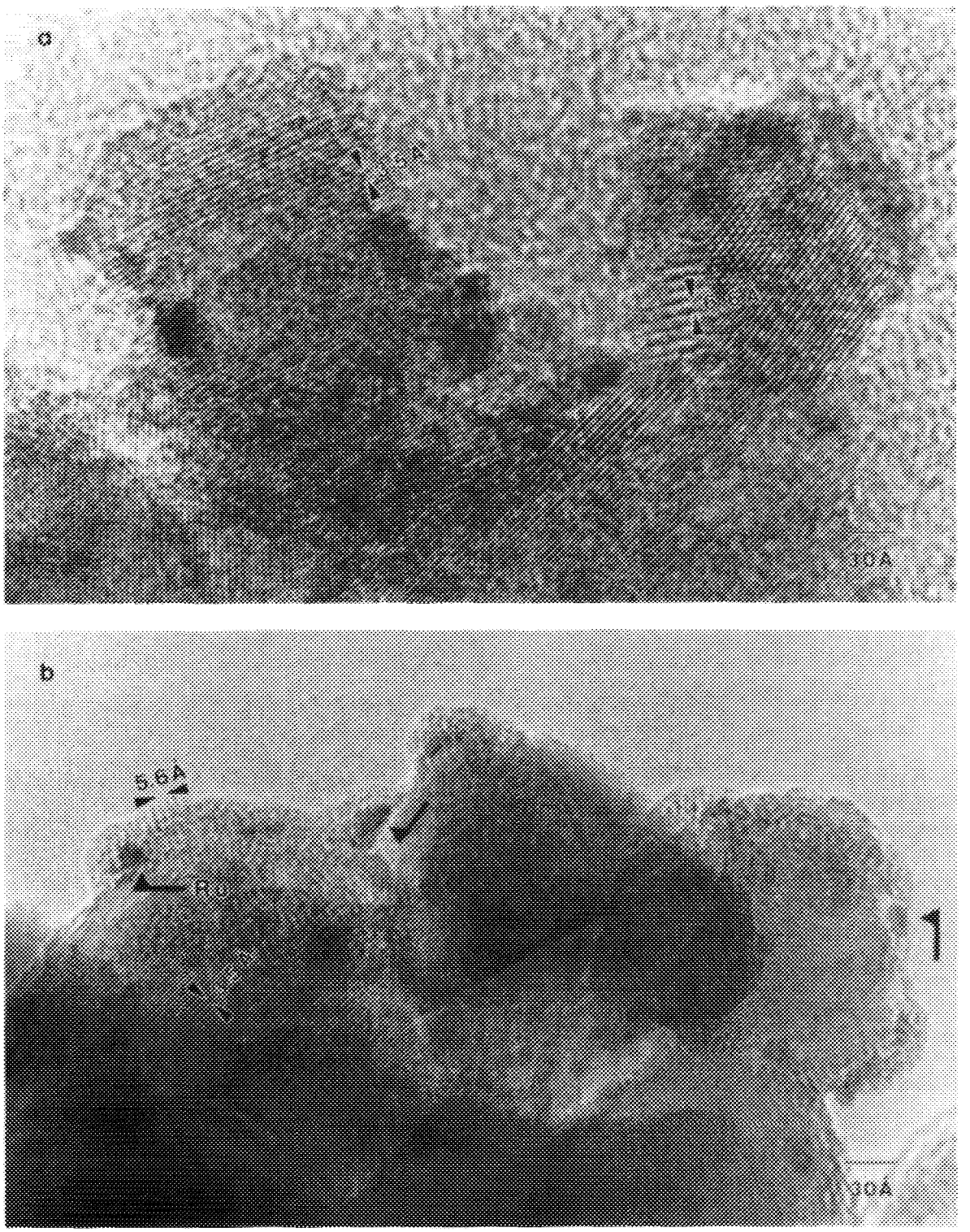

FIG. 1. High-resolution TEM images of Na-containing Ru/TiO_2 (sample C1). The arrows in image (a) identify a region in which the lattice fringe spacing is 3.5 Å, characteristic of anatase, and a strongly crystalline region with lattice fringe spacings of 6.6 Å. In image (b) a weakly crystalline oxide overlayer with 5.6 Å lattice fringe spacings is observed, fully encapsulating a Ru particle (black arrow) supported on anatase.

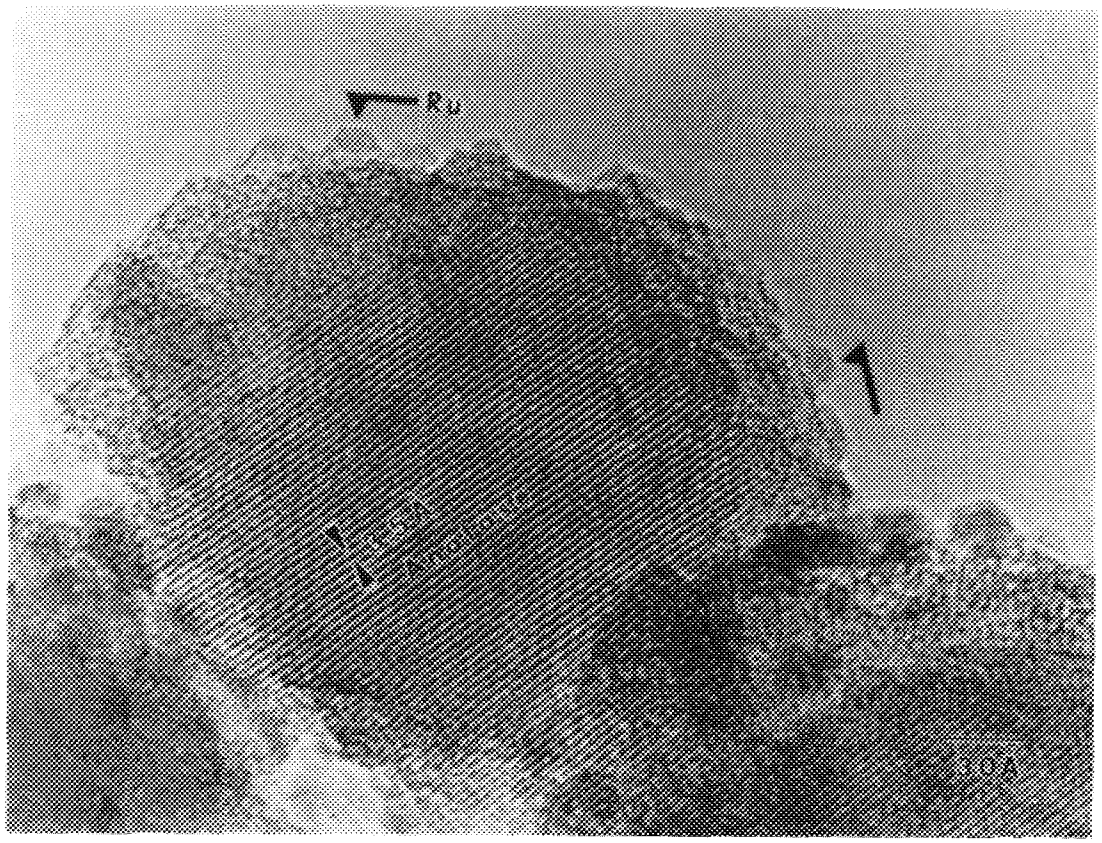

FIG. 2. A high-resolution TEM image of Na-free Ru/TiO_2 (sample C2). The faceted surfaces of the small Ru particles appear exposed.

at 573 K. In contrast, temperatures around 1123 K are required to form Na_2RuO_3 and Na_3RuO_4 (27).

The formation of sodium titanate phases facilitates the migration of Ti-containing moieties onto the Ru particles as a consequence of a reduction in the temperature for the onset of surface diffusion, which lies between $0.33T_m$ and $0.23T_m$, where T_m is the melting point (28, 29). Table 3 lists values of the melting points and the surface diffusion temperatures for anatase, rutile, and three sodium titanate phases. The lower melting points of the sodium titanates compared to anatase or rutile suggests that surface diffusion of Ti-containing moieties at 523 K, the catalyst-reduction temperature used in this study, will occur much more readily in the presence than in the absence of Na.

The effect of Na on the mobility of hydrogen on titania-supported Ru was investigated by means of selective excitation (hole burning) ^1H NMR (23). Figure 4 represents ^1H NMR spectra obtained under single-pulse and selective excitation after Na-free Ru/TiO_2 (sample A2) was exposed to hydrogen and evacuated to below 10^{-5} Torr. Hydrogen adsorbed on Ru exhibits a single resonance line at about -70 ppm, well separated from the NMR resonance representing hydrogen associated with titania. Selective excitation of a narrow frequency band was easily achieved within the upfield peak, showing inhomogeneous line broadening. A similar experiment performed at higher hydrogen coverage (Fig. 4, bottom) did not result in hole burning. The entire peak representing hydrogen on Ru was saturated indicating that the line became homogeneously broadened. As was demonstrated earlier (22, 23), the dipolar couplings between protons are negligibly small; therefore, the transition from inhomogeneous to homogeneous line broadening originates from increased hydrogen mobility. Analogous results for Na-containing Ru/TiO_2 (sample A1) are shown in Fig. 5a and 5b. Two peaks, A and B, are evident, both of which are associated with hydrogen on Ru. The location of peak B and its response to selective excitation are similar to what was previously observed for Na-free Ru/TiO_2. Under vacuum conditions, peak B is inhomogeneously broadened (Fig. 5a, bottom). At elevated pressures (>0.5 Torr), the broadening of this peak is dominated by a homogeneous mechanism revealed by the saturation of this resonance line under selective excitation (Fig. 5b, bottom). Peak A, on the other hand, does not undergo a transition to homogeneous line broadening and maintains its inhomogeneous character to a hydrogen pressure of at least 200 Torr. The response of the hydrogen spins in our selective excitation

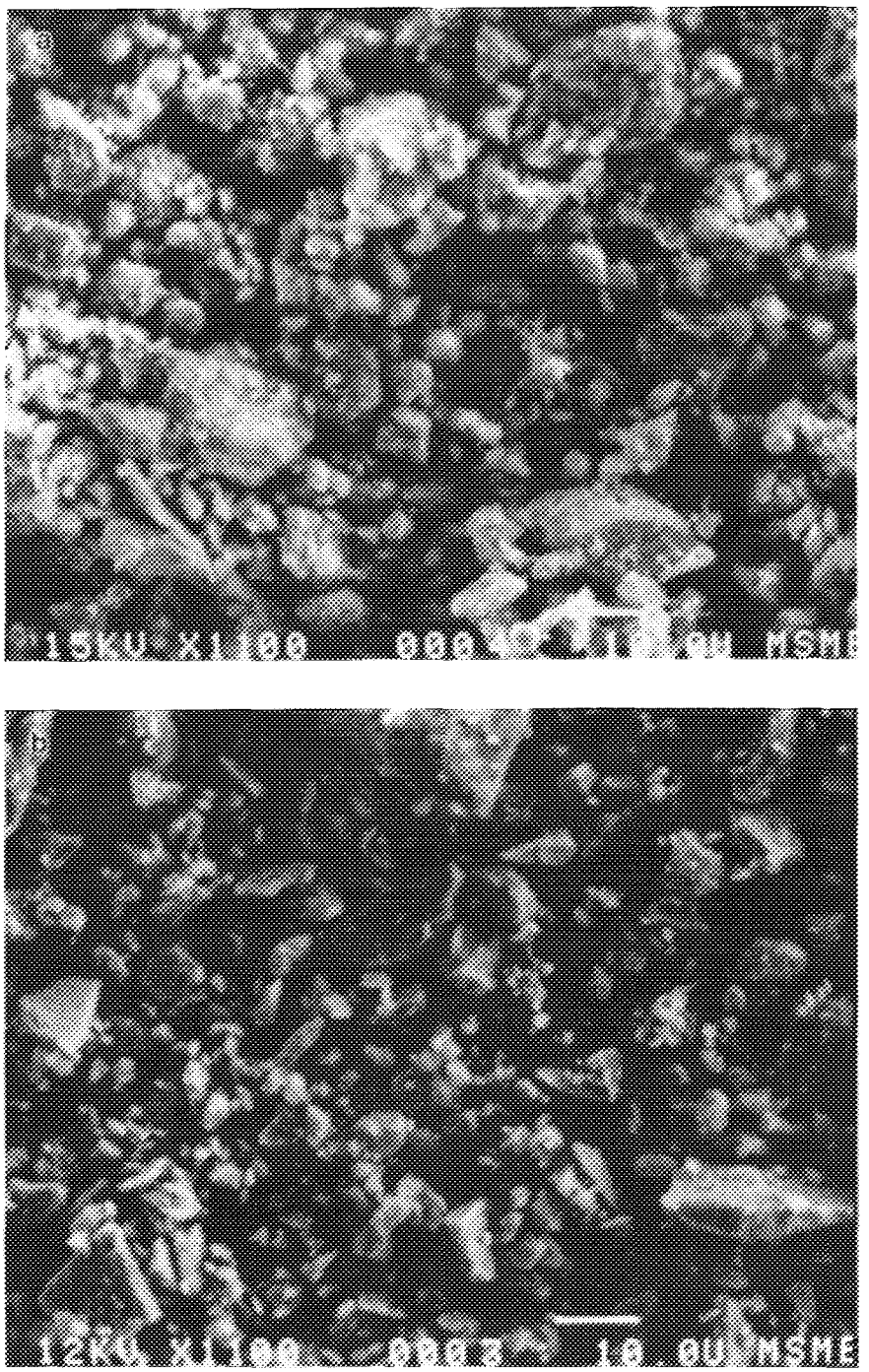

FIG. 3. SEM images of (a) Na-containing (C1) and (b) Na-free (C2) Ru/TiO_2.

experiments under elevated pressure indicates that the motion of hydrogen ascribed to peak A occurs within a time scale of ≥ 10 ms, while the motion of hydrogen ascribed to peak B is characterized by a much shorter time scale of ≤ 100 μs (22, 23). The interpretation of peak A has not yet been established. However, it can be concluded that it represents hydrogen interacting with Ru, but in the vicinity of Na, as revealed by the modified (lowered) Knight shift. Although the above analysis is only qualitative, it demonstrates that at least part of the hydrogen adsorbed on Na-containing Ru/TiO_2 exhibits decreased mobility.

TABLE 3

Melting Point and Surface Diffusion Temperature for Various Oxides

Oxide	T_m (K)	$0.23T_m$ (K)	$0.33T_m$ (K)
Na_2TiO_3	1303	510	613
$Na_2Ti_2O_5$	1258	500	598
$Na_2Ti_3O_7$	1401	532	645
TiO_2 (anatase)	1949	558	876
TiO_2 (rutile)	2030	600	885

Figure 6 illustrates the effects of Na on the turnover frequencies for CO consumption, N_{CO}, and the formation of methane, N_{CI}, during FTS. The abscissa in this plot is the enhancement in the extent of Ru surface coverage by Ti-containing moieties caused by the presence of Na. Both turnover frequencies presented on the ordinate of Fig. 6 are based on the Ru sites available for H_2 adsorption. The values of N_{CO} and N_{CI} are identical for the three Na-free samples (A2, B2, and C2). The presence of Na has relatively little effect on N_{CO} but causes a progressive decrease in N_{CI} with increasing concentration of Na (see Table 1).

The influence of Na content on the probability of chain growth, α, and the turnover frequencies for the formation of olefins and paraffins of given carbon number are presented in Figs. 7, 8, and 9, respectively. Figure 7 shows that with increasing Na content the value of α rises slightly. The presence of Na causes an increase in the

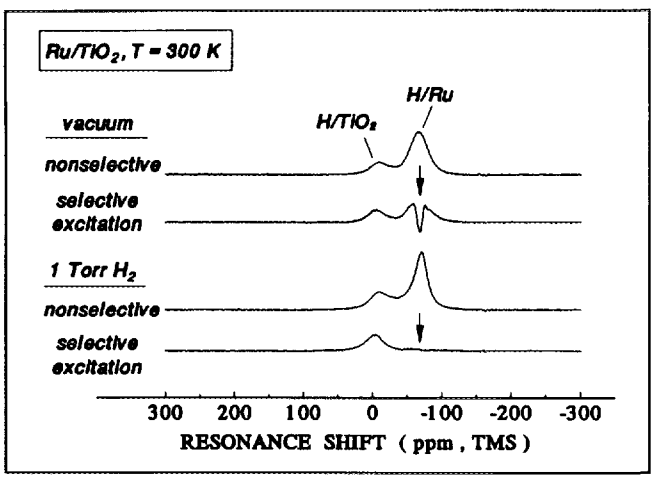

FIG. 4. ^1H NMR spectra of hydrogen on Ru/TiO_2 (sample A2) at ambient temperature. Top: Spectra obtained under evacuation conditions by nonselective excitation. Bottom: Spectra obtained under external hydrogen pressure of 1 Torr by nonselective and selective excitation. The arrows mark the position of the carrier frequency in the selective-excitation experiments.

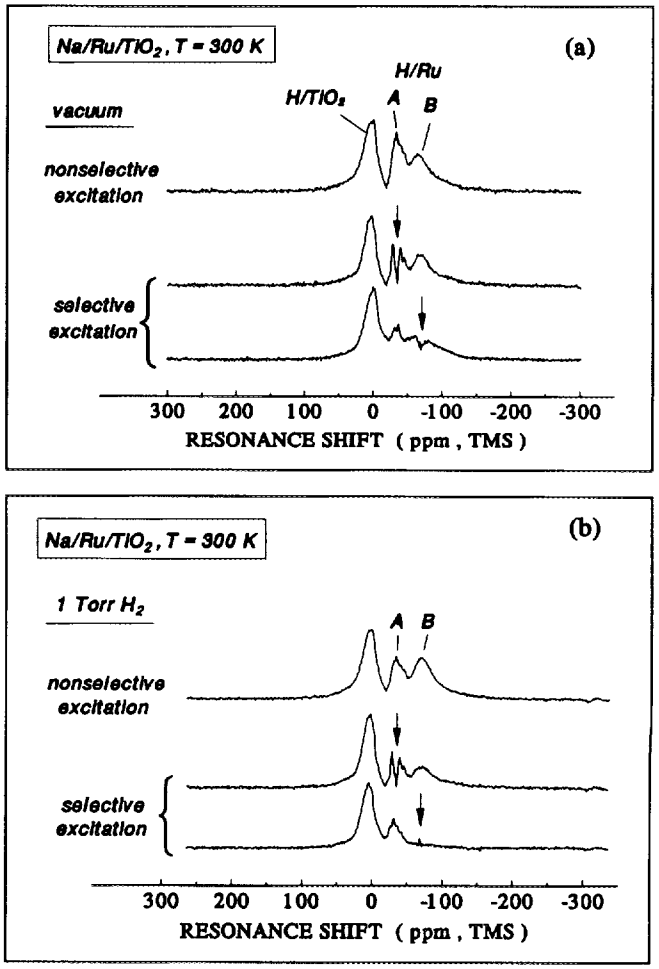

FIG. 5. ^1H NMR spectra of hydrogen on Na-containing Ru/TiO_2 (sample A1) at ambient temperature. The spectra were obtained by nonselective and selective excitation under vacuum conditions (a) and 1 Torr hydrogen (b). The arrows indicate the irradiation frequencies used in the selective-excitation experiment.

turnover frequencies for the formation of C_2 (Fig. 6) and C_4 (Fig. 9) olefins and a decrease in the turnover frequencies for the formation of the corresponding paraffins. It is interesting to note that for both C_2 and C_4 products the sum of olefin and paraffin turnover frequencies remains essentially constant, suggesting that the presence of Na suppresses the rate of olefin hydrogenation, but has little effect on the rate of forming products with a given carbon number.

Table 4 reports the effects of adding ethylene to the freedstream. To distinguish the source of carbon, ^{13}CO and $^{12}C_2H_4$ are used. It is apparent that the presence of Na decreases the extent of ethylene incorporation into the C_{3+} products. The fraction of ^{12}C in the C_{3+} products can be represented by the formula $[2f_i + (n - 2)f_m]/n$, where f_i and f_m are the fraction of chain initiators and the

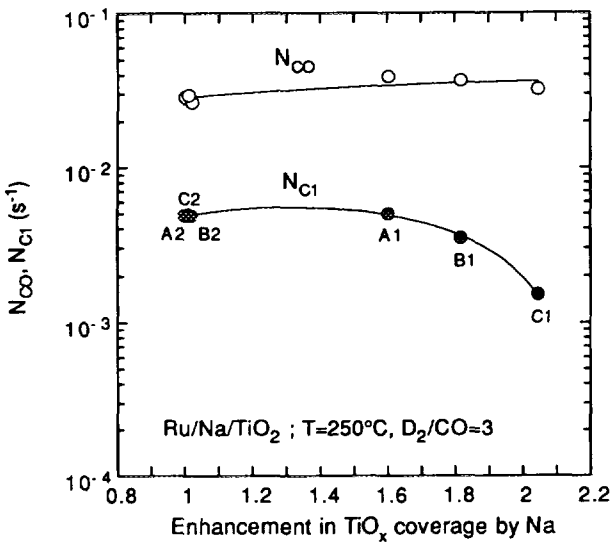

FIG. 6. Turnover frequencies for CO consumption (N_{CO}) and methane formation (N_{C1}) as a function of the enhancement in Ru surface coverage by Ti-containing moieties. Both turnover frequencies are based on the number of Ru sites available for H_2 chemisorption, as determined from ^1H NMR.

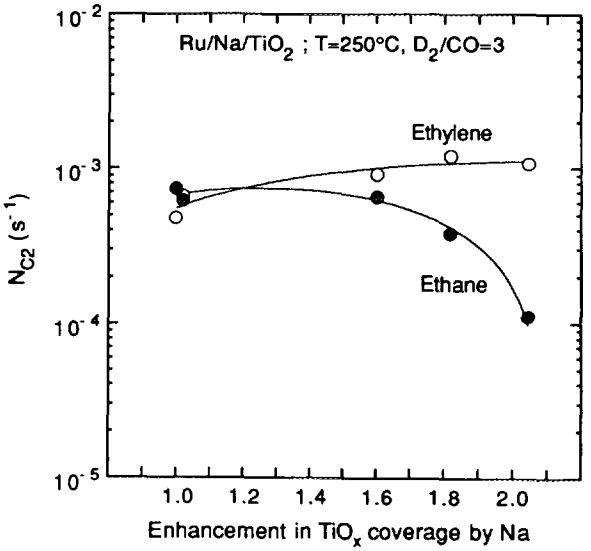

FIG. 8. Turnover frequencies for the formation of ethylene and ethane as a function of the enhancement in Ru surface coverage by Ti-containing moieties. Both turnover frequencies are based on the number of Ru sites available for H_2 chemisorption, as determined from ^1H NMR.

fraction of monomer units derived from $^{12}C_2H_4$, respectively (30). Table 4 demonstrates that the values of f_i and f_m both decrease in the presence of Na.

It is interesting to compare the results of the present investigation with those of Komaya *et al.* (10), who investigated the effects of TiO_x coverage on the activity and selectivity of Na-free Ru/TiO_2 for Fischer–Tropsch synthesis. In that study, it was observed that N_{CO} passes through a maximum for $\theta_{TiO_x} > 0.5$, whereas N_{C1} decreases monotonically with increasing values of θ_{TiO_x}. The probability of chain growth and the olefin-to-paraffin ratio of the products both increase with θ_{TiO_x}. The effects of an increase in the coverage of the Ru particle surface by Ti-containing species, observed in the present study, are similar in all respects but one to those reported by Komaya *et al.* (10) for $\theta_{TiO_x} > 0.5$. The only difference is that

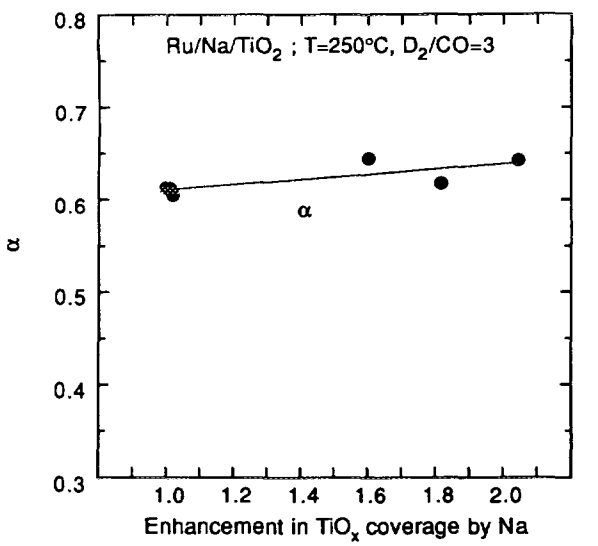

FIG. 7. Probability of chain growth (α) as a function of the enhancement in Ru surface coverage by Ti-containing moieties.

TABLE 4

Fraction of ^{12}C in the Hydrocarbon Products Formed from a Feed Containing $^{12}C_2H_4$ (1.17%)/^{13}CO (10%)/H_2 (30%)/He (Bal.)[a]

$F_n(^{12}C)$	Na-free Ru/TiO_2 (C2)		Na-containing Ru/TiO_2 (C1)	
	Exp.	*Sim.*[b]	*Exp.*	*Sim.*[b]
C_3	0.69	0.73	0.44	0.46
C_4	0.63	0.59	0.38	0.37
C_5	0.53	0.50	0.34	0.31
C_6	0.45	0.44	0.26	0.27
C_7	0.38	0.39	0.21	0.24
C_8	—	—	0.22	0.22
f_m	0.14		0.07	
f_i	1.03		0.66	

[a] Reaction conditions: T = 523 K; P = 1 atm; τ_b = 0.23 s.

[b] $F_n(^{12}C) = 1/n\,[2f_i + (n-2)f_m]$, where f_m is the fraction of ^{12}C-labeled C_1 monomer species and f_i is the fraction of ^{12}C-labeled C_2 initiator in the C_{3+} products (27).

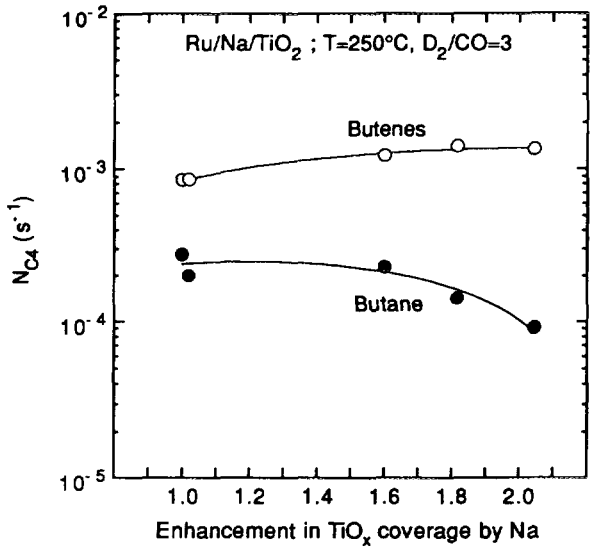

FIG. 9. Turnover frequencies for the formation of butene and butane as a function of the enhancement in Ru surface coverage by Ti-containing moieties. Both turnover frequencies are based on the number of Ru sites available for H_2 chemisorption, as determined from ^1H NMR.

when the increase in Ru particle coverage by Ti-containing moieties is driven by increasing concentration of Na, the value of N_{CO} remains nearly constant (see Fig. 6).

The effects of increasing coverage of Ru particles by Ti-containing species on N_{C1}, α, and the olefin-to-paraffin ratio can all be attributed to a reduction in the adsorption of H_2 and/or the surface mobility of adsorbed H atoms. Previous studies (17, 18) have shown that the promotion of transition metals by alkali metal oxides inhibits the adsorption of H_2, and as discussed above, selective excitation ^1H NMR experiments indicate that in the presence of Na, the mobility of at least a portion of the adsorbed hydrogen is reduced.

A further consequence of the lower abundance of adsorbed H atoms on the Na-containing samples is the reduced participiation of product ethylene in the initiation and propagation of hydrocarbon chains (see Table 4). Chain initiation by readsorbed ethylene requires the formation of ethyl groups via the reaction $C_2H_{4,s} + H_2 \rightarrow C_2H_{5,s}$. Clearly, this process depends upon the availability of adsorbed H atoms. The formation of $CH_{2,s}$ species from readsorbed ethylene is energetically favored via the process $C_2H_{5,s} \rightarrow CH_{3,s} + CH_{2,s}$ (31, 32). Inhibition of the formation of ethyl species will reduce the rate at which new methylene species are formed.

The near constancy of N_{CO} with increasing coverage of the Ru particles by Ti-containing species is more difficult to understand. Promotion of Ru/SiO_2 with alkali metal oxides causes a monotonic decrease in N_{CO} with increased alkali loading. A similar trend is observed for TiO_x on Ru for $\theta_{TiO_x} > 0.5$ (10). In view of these results, one can only suggest that the behavior of N_{CO} seen in Fig. 6 must be attributable to the effects of Na on the physicochemical properties of the Ti-containing species covering the surface of Ru. It should be noted that the increased coverage in Ti-containing species is achieved by increasing the weight loading of Na in the sample (see Table 1) and, as a consequence, the metal oxide overlayer on the surface of the Ru particles is expected to be progressively more Na-rich as one moves from left to right along the abscissa of Fig. 6.

The results of the present work demonstrate that the coverage of Ru particles supported on TiO_2 is very sensitive to alkali metals present as impurities in either the support or the metal precursor. In good agreement with the suggestion of Spencer (19), alkali metals (e.g., Na, K) can react with titania to form small quantities of alkali metal titanates. These materials exhibit much lower melting points than titania and, hence, can migrate by surface diffusion at a much lower temperatures than pure titania (anatase or rutile). Differences in the content of alkali metal in different titania-supported transition metal catalysts could account for reported differences in the effects of a given metal oxide promoter on the FTS activity and selectivity of the metal. Since the coverage of metal particles by Ti-containing moieties can now be determined quantitatively, it is possible to ascertain the specific effects of oxide overlayer coverage on the catalytic properties of a metal.

CONCLUSIONS

Sodium is found to facilitate the migration of Ti-containing moieties onto the surface of Ru particles supported on titania, the extent of this effect increasing with the content of Na in the sample. This role of Na is attributed to the formation of sodium titanate phases for which the melting point and, hence, the minimum temperature for surface migration are lower than those for the anatase or rutile phases of titania. Increasing surface coverage of the Ru particles by Ti-containing moieties causes a small increase in the probability of chain growth, a modest increase in the olefin-to-paraffin ratio of the products, and a decrease in the reincorporation of product ethylene, but has little effect on the turnover frequency for CO consumption during FTS. All three of these effects might be attributable to a reduction in the mobility of adsorbed H atoms.

ACKNOWLEDGMENTS

This work was supported by the Office of Chemical Sciences, Division of Basic Energy Sciences, of the U.S. Department of Energy under Contract DE-AC03-76SF00098 at the Lawrence Berkeley Laboratory and under Contract W-7405-Eng-82 at the Ames Laboratory. Access to the facilities at the National Center for Electron Microscopy is acknowl-

edged. Z. Weng-Sieh gratefully recognizes support through a Noyce Foundation fellowship.

REFERENCES

1. Anderson, R. B., "The Fischer–Tropsch Syntheses," Wiley, New York, 1984.
2. Tauster, S. J., *Acc. Chem. Res.* **20,** 389 (1987).
3. Bell, A. T., *in* "Catalyst Design—Progress and Perspectives" (L. L. Hegedus, Ed.), Wiley, New York, 1987.
4. Burch, R., *in* "Hydrogen Effects in Catalysis" (Z. Paal and P. G. Menon, Eds.), Dekker, New York, 1988.
5. Haller, G. L., and Resasco, D. E., *Adv. Catal.* **36,** 173 (1989).
6. Vannice, M. A., *Catal. Today* **12,** 255 (1992).
7. Burch, R., and Flambard, A. R., *J. Catal.* **86,** 384 (1982).
8. Sachtler, W. M. H., Shriver, D. F., Hollenberg, W. B., and Lang, A. F., *J. Catal.* **92,** 429 (1985).
9. Komaya, T., Bell, A. T., Weng-Sieh, Z., Gronsky, R., Engelke, F., King, T. S., and Pruski, M., *J. Catal.* **149,** 142 (1994).
10. Komaya, T., Bell, A. T., Weng-Sieh, Z., Gronsky, R., Engelke, F., King, T. S., and Pruski, M., *J. Catal.* **150,** 400 (1994).
11. Gonzalez, R. D., and Miura, H., *J. Catal.* **77,** 338 (1982).
12. McClory, M. M., and Gonzalez, R. D., *J. Catal.* **89,** 392 (1984).
13. Mori, T., Miyamoto, A., Niizuma, H., Hattori, H., and Murakami, Y., *React. Kinet. Catal. Lett.* **26,** 335 (1984).
14. Okuhara, T., Tamura, H., and Misono, M., *J. Catal.* **95,** 41 (1985).
15. Mori, T., Miyamoto, A., Takahashi, H., Niizuma, H., Hattori, H., and Murakami, Y., *J. Catal.* **102,** 199 (1986).
16. Hoost, T. E., and Goodwin, J. G., Jr., *J. Catal.* **137,** 22 (1992).
17. Hoost, T. E., and Goodwin, J. G., Jr., *J. Catal.* **130,** 283 (1991).
18. Uner, D. O., Pruski, M., Gerstein, B. C., and King, T. S., *J. Catal.* **146,** 530 (1994).
19. Spencer, M. S., *J. Phys. Chem.* **88,** 1046 (1984).
20. Morris, G. A., and Freeman, R., *J. Magn. Reson.* **29,** 433 (1978).
21. Haddix, G. W., Reimer, J. A., and Bell, A. T., *J. Catal.* **106,** 111 (1987).
22. Engelke, F., Vincent, R., King, T. S., and Pruski, M., *J. Phys. Chem.* **101,** 7262 (1994).
23. Engelke, F., Bhatia, S., King, T. S., and Pruski, M., *Phys. Rev. B* **49,** 2730 (1994).
24. Komaya, T., and Bell, A. T., *J. Catal.* **146,** 237 (1994).
25. Andersson, S., and Wadsley, A. D., *Acta Crystallogr.* **15,** 201 (1962).
26. Watanabe, T., *J. Solid State Chem.* **36,** 91 (1986).
27. Shaplygin, I., and Lazarev, V. B., *Russ. J. Inorg. Chem.* **25,** 1837 (1980).
28. Gray, T. J., "Solid State," *in* "Encyclopedia of Chemical Technology" (R. E. Kirk and D. F. Othmer, Eds.), First Supplement Volume, pp. 828–837. Interscience Encyclopedia, New York, 1957.
29. Huttig, G., *Discus. Faraday Soc.* **8,** 215 (1950).
30. Krishna, K. R., and Bell, A. T., *Catal. Lett.* **14,** 305 (1992).
31. Shustorovich, E., and Bell, A. T., *Surf. Sci.* **121,** 359 (1991).
32. Bell, A. T., *in* "Metal–Surface Reaction Energetics—Theory and Applications to Heterogeneous Catalysis, Chemisorption, and Surface Diffusion" (E. Shustorovich, Ed.), VCH, New York, 1991.